Available online at www.sciencedirect.com
ScienceDirect
Journal of the Chinese Medical Association 80 (2017) 109−116
www.jcma-online.com

Original Article

Patterns of cerebrospinal fluid (CSF) distribution in patients with spontaneous intracranial hypotension: Assessed with magnetic resonance myelography

Chuan-Han Chen [a], Jeon-Hor Chen [b,c], Hung-Chieh Chen [a,*], Jyh-Wen Chai [a], Po-Lin Chen [d], Clayton Chi-Cheng Chen [a]

[a] *Department of Radiology, Taichung Veterans General Hospital, Taichung, Taiwan, ROC*
[b] *Tu and Yuen Center for Functional Onco-Imaging and Department of Radiological Science, University of California, Irvine, USA*
[c] *Department of Radiology, E-Da Hospital and I-Shou University, Kaohsiung, Taiwan, ROC*
[d] *Department of Neurology, Taichung Veterans General Hospital, Taichung, Taiwan, ROC*

Received November 23, 2015; accepted February 16, 2016

Abstract

Background: Diagnosis of spontaneous intracranial hypotension (SIH) relies on the ability of medical staff to recognize cerebrospinal fluid (CSF) leakage at the spine. However, difficulties with interobserver discrepancy sometimes occurred while reading magnetic resonance myelography (MRM) because clear image definition was lacking. In this study, we tried to determine which pattern of CSF distribution is more reliable for diagnosis of CSF leakage by using MRM.

Methods: From January 2012 to August 2014, 19 SIH patients and 27 healthy controls (HC) were recruited into our study; 10 of the 19 patients were recovered (SIH-R) after treatment. Whole spine MRM was performed using the 3D-SPACE (three-dimensional sampling perfection with application-optimized contrasts using different flip-angle evolutions) sequence, and interpreted by two experienced neuroradiologists. Two 4-point classification systems of CSF distribution were used to evaluate the three-dimensional maximum intensity projection (3D MIP) and the thin-slice axial multiplanar reconstruction (MPR) images, respectively.

Results: The interobserver agreement between the two readers interpreting the 3D MIP and thin-slice axial MPR MRM were moderate to good ($\kappa = 0.60-0.78$). Grade 3 of 3D MIP and Type D of axial MPR MRM were only noticed in the SIH. Overall, Grade 3 of MIP and Type D of MPR showed significant difference ($p < 0.008$) between the SIH and the HC in the whole spine. Type C at the T-spine was more frequently noted in the SIH than in the HC ($p < 0.038$). By using "Grade 3", "Type D", "Type D and Type C at T-spine" as the diagnostic criteria of CSF leakage, the sensitivity, specificity, positive predict value (PPV), and negative predict value (NPV) were all > 70%.

Conclusion: Grade 3 on 3D MIP and Type D on axial MPR MRM were definite criteria of MRM for localizing CSF leakage, and Type C in the T-spine was a probable leakage sign with high sensitivity and NPV.
Copyright © 2016, the Chinese Medical Association. Published by Elsevier Taiwan LLC. This is an open access article under the CC BY-NC-ND license (http://creativecommons.org/licenses/by-nc-nd/4.0/).

Keywords: cerebrospinal fluid; magnetic resonance myelography; spontaneous intracranial hypotension

1. Introduction

Spontaneous intracranial hypotension (SIH), a disease caused by cerebrospinal fluid (CSF) leakage at the level of the spine, is known for its prototypical symptom of orthostatic headache. The annual incidence of this disease is about five per 100,000.[1] However, SIH may be misdiagnosed because of

Conflicts of interest: The authors declare that they have no conflicts of interest related to the subject matter or materials discussed in this article.

* Corresponding author. Dr. Hung-Chieh Chen, Department of Radiology, Taichung Veterans General Hospital, 1650, Section 4, Taiwan Boulevard, Taichung 407, Taiwan, ROC.
E-mail address: hungchiehchen@gmail.com (H.-C. Chen).

http://dx.doi.org/10.1016/j.jcma.2016.02.013
1726-4901/Copyright © 2016, the Chinese Medical Association. Published by Elsevier Taiwan LLC. This is an open access article under the CC BY-NC-ND license (http://creativecommons.org/licenses/by-nc-nd/4.0/).

atypical clinical presentations.[2] If left untreated, complications may occur, such as subdural hemorrhage, brain herniation, and death. Therefore, accurate and prompt diagnosis of SIH is crucial for successful treatment.

Detection of the CSF leakage site in the spine is important for diagnosis and treatment of SIH,[3] especially for patients who require an epidural blood patch (EBP). Although targeted EBP is not always necessary,[4] placing a blood patch at the leakage site is generally considered more effective than placing it at a distant site, and this approach usually provides long-term relief.[5] Imaging modalities that have been used to detect CSF leakage in the spine include computed tomographic myelography (CTM), radioisotope cisternography (RIC), and magnetic resonance myelography (MRM). As a radiation-free and noninvasive imaging method, MRM is the first choice for many clinicians.[6,7] Commonly-reported MRM findings indicating the location of CSF leakage include a triangular-shaped expansion of the neural sleeve and an irregular linear signal lateral to the neural sleeve, representing a periradicular leak.[8,9] Epidural fluid collection is the imaging finding for diagnosis, but not for localization of CSF leakage. However, there is no clear definition of these imaging findings, such as what degree of triangular expansion is meaningful or what length of linear signal around the nerve sleeve indicates a periradicular leak. Occasionally, CSF leaks are not detected, yielding false negatives, and MRM images in the normal population may indicate CSF leakage, yielding false positives.[10] These are the major reasons for interobserver discrepancy in MRM image interpretation.

Only one report in the literature has defined the CSF distribution pattern in SIH. In that study, the authors used two-dimensional maximum intensity projection (2D MIP) MRM to diagnose CSF leakage with 80–93% sensitivity and specificity.[6] However, the grading system was not applied to evaluate MRMs of healthy controls. In addition, for targeted EBP, thin-slice axial multi-planar reconstruction (MPR) MRM is usually required. A new grading system is necessary for thin-slice axial MPR MRM, which can differentiate SIH patients from healthy controls and accurately identify the CSF leakage site. Therefore, the current study aimed to determine which pattern of CSF distribution on thin-slice axial MPR MRM images is most reliable for diagnosis of CSF leakage and to develop a new grading system.

2. Methods

2.1. Participants

By retrospectively reviewing electronic charts from January 2012 to August 2014, we selected 19 patients who were diagnosed with SIH (according to Schievink criteria[3] or the International Classification of Headache Disorders, 3rd Edition[11]) and treated in the neurology ward. During their hospital stay, patients received conservative treatment and targeted epidural blood patch (EBP). Whole spine MRM images from initial hospitalization and after complete recovery were reviewed. Complete recovery was defined as patients having no more headaches or other associated orthostatic symptoms.

A total of 27 healthy volunteers with no known neurological disorders, spine malformations, or previous spine operations were recruited in this study as healthy controls (HC), and whole spine MRM was performed for each individual. No pathological findings were accepted in MR images except minor degenerative changes of the spine.

Prior to enrollment, written informed consent was obtained from all participants; this study was approved by the Institutional Review Board (IRB) of Taichung Veterans General Hospital, Taichung, Taiwan.

2.2. Magnetic resonance myelography

Participants underwent MRM imaging of the whole spine in a 1.5T magnetic resonance imaging (MRI) scanner (MAGNETOM Aera, Siemens Healthcare, Erlangen, Germany) using three-dimensional sampling perfection with application of optimized contrasts using different flip-angle evolutions (3D-SPACE) sequences. The parameters were as follows: The repetition time (TR) 3000 ms, The echo time (TE) 560 ms, fat suppression, isotropic voxel size 0.9 mm, matrix size 320 × 320, and field of view (FOV) 200 mm. The generalized auto-calibrating partially parallel acquisitions (GRAPPA) imaging reconstruction technique with an acceleration factor of 2 was used. Images were volumetrically acquired in the coronal plane of the C-T and T-L spine, parallel to the spinal curve with some overlapping. Total acquisition time was 12 minutes. Thin-slice axial MPR images were reconstructed with a slice thickness of 5 mm, and three-dimensional (3D) MIP images were reconstructed at the cervical (C-), thoracic (T-), and lumbar (L-) spinal segments for image evaluation.

2.3. Image evaluation

We evaluated the 3D MIP MRM images using a 4-point grading system (Grade 0–3), which was proposed by Yoo et al[6] (Fig. 1). The longest neural sleeve observed at different

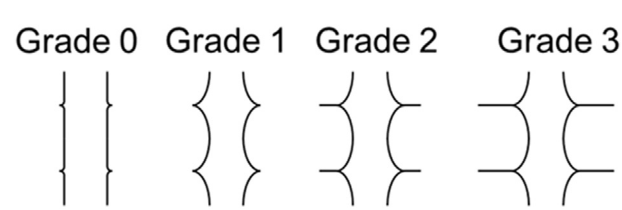

Fig. 1. Schematic diagram of the 4-point grading system for imaging appearance of CSF on three-dimensional MIP MRM images. Grade 0, no CSF expansion from the CSF space column; Grade 1, unilateral or bilateral triangular-shaped expansion of CSF space column around the nerve root sleeve; Grade 2, high signal intensity stripe with length less than the width of the thecal sac, arising from a unilateral or bilateral triangular-shaped expansion of CSF space column around the nerve root sleeve; Grade 3, high signal intensity stripe with the length greater than the width of the thecal sac, arising from a unilateral or bilateral triangular-shaped expansion of CSF space column around the nerve root sleeve. CSF = cerebrospinal fluid; MIP = maximum intensity projection; MRM = magnetic resonance myelography.

spinal segments was used for categorization. As the thin-slice axial MPR MRM images were crucial to localize the leakage site, we created a classification system (Type A–D) to evaluate thin-slice axial MPR MRM images (Fig. 2), based on the Yoo et al's[6] MIP grading scale. All images were viewed on a picture archiving and communication system (PACS). MRM images were evaluated by two neuroradiologists with 5 years and 10 years of experience in reading MRI who were blinded to the clinical conditions of this study. C-, T-, and L-spinal segments were analyzed. The C7-T1 level was defined as T-spine, and the T12-L1 level was defined as L spine. The presence of epidural fluid or C1-2 fluid accumulation was also recorded.

2.4. Statistical analysis

Data were analyzed using the program SPSS (version 18; SPSS Inc., Chicago, IL, USA). Demographic data, patterns of CSF distribution, and presence of epidural fluid were compared between the participants. Interobserver agreement was evaluated between the two readers using the kappa coefficient (κ). The Kolmogorov–Smirnov test was used to verify normal distribution of continuous variables. The ages of SIH and HC patients did not have a normal distribution and were therefore analyzed using a nonparametric Mann–Whitney *U* test. Fisher's exact test was used for nominal variables. All tests were two-tailed, and the level of statistical significance was set at $p < 0.05$.

3. Results

Our study included 19 SIH patients (13 female and 6 male; mean age, 38.2 years) and 27 individuals in the HC group (17 female and 10 male; mean age, 36.3 years). We found there were no significant group differences in sex or age. Among the 19 SIH patients, 10 recovered completely and were categorized as the SIH recovery (SIH-R) group (8 female and 2 male; mean age, 37.7 years); five patients received one EBP, and the other five patients received two EBPs before complete recovery. Demographic data are shown in Table 1.

Interobserver agreements between the two readers for interpreting thin-slice axial MPR MRM were good in SIH patients (κ = 0.74) and HC participants (κ = 0.75). Interobserver agreements for interpreting 3D MIP MRM was good in SIH patients (κ = 0.72), but only moderate in HC participants (κ = 0.6).

3.1. Patterns of CSF distribution on MRM

To determine which MRM findings are most reliable for CSF leakage, we evaluated CSF distribution patterns and the presence or absence of epidural fluid in SIH and HC participants at C-, T- and L-spinal segments.

3.1.1. Three-dimensional MIP MRM images

The results of two readers interpreting 3D MIP MRM images using the grading system at different spinal segments are shown in Table 2. Data are presented as number and percentage of participants. Actually, results were similar between the two readers. Grade 3 was observed only in the SIH group, and significant differences were observed between SIH and HC in C-, T- and L-spine by Reader 2, and in C- and T-spine by Reader 1. Grade 3 was also significantly different between the SIH and SIH-R groups at C-and T-spine by Reader 1. Although there were no significant differences at L-spine by Reader 1 or at any segments by Reader 2, none of the SIH-R group had Grade 3 imaging patterns on 3D MIP MRM. Compared with the HC participants, SIH patients showed significantly less Grades 0 or 1 in T-spine, and less Grade 1 in C-spine.

3.1.2. Thin-slice axial MPR MRM images

Table 3 shows the results of two readers interpreting thin-slice axial MPR MRM images using the grading system at different spinal segments. Data are presented as numbers and percentages of participants. Again, similar results were noted between the two readers. Type D was only observed in SIH patients; it was more frequent in the SIH group than in the HC group across all spinal segments and in the SIH group than in the SIH-R group at the T-spine. Type C was more frequent in the SIH group than in the HC group at both T- and L-spine,

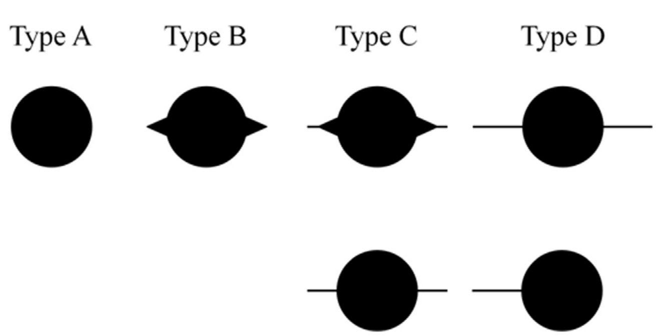

Fig. 2. Schematic drawing of 4-type classification of imaging appearance of CSF on thin-slice axial MPR MRM images. Type A, no CSF expansion from the thecal sac; Type B, unilateral or bilateral triangular-shaped expansion of the CSF space around the nerve root sleeve of the thecal sac; Type C, high signal intensity stripe with length less than the width of the thecal sac, unilateral or bilateral to the nerve root sleeve, with or without triangular-shaped expansion of the CSF space; Type D, high signal intensity stripe with length more than the width of the thecal sac, unilateral or bilateral to the nerve root sleeve, with or without triangular-shaped expansion of the CSF space. CSF = cerebrospinal fluid.

Table 1
Demographic data.

	HC	SIH	*p*
Age (y)	36.26 (10.6)	38.2 (11.22)	0.77
Range	20–50	23–59	
Sex			
Male	10	6	0.76
Female	17	13	

Data are presented as *n* or mean (standard deviation), unless otherwise indicated.
HC = healthy controls; SIH = spontaneous intracranial hypotension.

Table 2
Grading of three-dimensional MIP MRM by group and spinal segment from Readers 1 and 2.

Spinal segment	Grade	HC ($n = 27$)	SIH ($n = 19$)	SIH-R ($n = 10$)	HC vs SIH	SIH vs SIH-R
Reader 1						
C-spine	0	1 (3.7)	1 (5.2)	0 (0)	1.000	1.000
	1	17 (63.0)	4 (21.1)	5 (50)	0.007	0.205
	2	9 (33.3)	6 (31.6)	5 (50)	1.000	1.000
	3	0 (0.0)	8 (42.1)	0 (0)	< 0.001	0.027
T-spine	0	10 (37.0)	1 (5.2)	3 (30)	0.016	0.105
	1	13 (48.2)	1 (5.2)	4 (40)	0.003	0.036
	2	4 (14.8)	6 (31.6)	3 (30)	0.277	1.000
	3	0 (0.0)	11 (58.0)	0 (0)	< 0.001	0.003
L-spine	0	8 (29.6)	4 (21.1)	3 (30)	0.735	0.665
	1	12 (44.5)	3 (15.8)	1 (10)	0.058	1.000
	2	7 (25.9)	9 (47.3)	6 (60)	0.209	0.700
	3	0 (0.0)	3 (15.8)	0 (0)	0.064	0.532
Reader 2						
C-spine	0	0 (0.0)	0 (0.0)	0 (0.0)	—	—
	1	20 (74.1)	5 (26.3)	7 (70.0)	0.002	0.046
	2	7 (25.9)	8 (42.1)	3 (30.0)	0.341	0.694
	3	0 (0.0)	6 (31.6)	0 (0.0)	0.003	0.068
T-spine	0	7 (25.9)	0 (0.0)	2 (20.0)	0.031	0.111
	1	12 (44.5)	1 (5.3)	3 (30.0)	0.006	0.105
	2	8 (29.6)	9 (47.3)	5 (50.0)	0.352	1
	3	0 (0.0)	9 (47.3)	0 (0.0)	< 0.001	0.11
L-spine	0	7 (26.0)	3 (15.8)	3 (30.0)	0.488	0.633
	1	10 (37.0)	4 (21.1)	3 (30.0)	0.335	0.665
	2	10 (37.0)	7 (36.8)	4 (40.0)	1	1
	3	0 (0.0)	5 (26.3)	0 (0.0)	0.008	0.134

Data are presented as *n* (%).
HC = healthy controls; MIP = maximum intensity projection; MRM = magnetic resonance myelography; SIH = spontaneous intracranial hypotension; SIH-R = spontaneous intracranial hypotension after recovery.

Table 3
Types of thin-slice axial MPR MRM images by group and spinal segment from Readers 1 and 2.

Spinal segment	Type	HC ($n = 27$)	SIH ($n = 19$)	SIH-R ($n = 10$)	HC versus SIH	SIH versus SIH-R
(a) Reader 1						
C-spine	A	27 (100.0%)	18 (94.7%)	9 (90.0%)	0.413	1.000
	B	27 (100.0%)	19 (100.0%)	10 (100.0%)	—	—
	C	7 (25.9%)	8 (42.1%)	4 (40.0%)	0.405	1.000
	D	0 (0.0%)	5 (26.3%)	0 (0.0%)	0.008	0.134
T-spine	A	27 (100.0%)	14 (73.7%)	9 (90.0%)	0.008	0.633
	B	23 (85.2%)	17 (89.5%)	10 (100.0%)	1.000	0.532
	C	7 (25.9%)	16 (84.2%)	4 (40.0%)	< 0.001	0.032
	D	0 (0.0%)	15 (78.9%)	0 (0.0%)	< 0.001	< 0.001
L-spine	A	23 (85.2%)	13 (68.4%)	8 (80.0%)	0.277	0.675
	B	19 (70.3%)	12 (63.2%)	5 (50.0%)	0.846	0.694
	C	7 (25.9%)	13 (68.4%)	6 (60.0%)	0.010	0.700
	D	0 (0.0%)	5 (26.3%)	0 (0.0%)	0.008	0.134
Spinal segment	**Type**	**HC ($n = 27$)**	**SIH ($n = 19$)**	**SIH-R (n = 10)**	**HC vs SIH**	**SIH vs SIH-R**
(b) Reader 2						
C-spine	Type A	27 (100.0%)	18 (94.7%)	10 (100.0%)	0.413	1
	Type B	27 (100.0%)	19 (100.0%)	9 (90.0%)	—	0.345
	Type C	3 (11.1%)	14 (73.7%)	10 (100.0%)	0.001	0.134
	Type D	0 (0.0%)	6 (31.6%)	0 (0.0%)	0.003	0.068
T-spine	Type A	27 (100.0%)	14 (73.7%)	9 (90.0%)	0.008	0.633
	Type B	21 (77.8%)	16 (84.2%)	9 (90.0%)	0.716	1
	Type C	5 (18.5%)	18 (94.7%)	6 (60.0%)	< 0.001	0.036
	Type D	0 (0.0%)	14 (73.7%)	0 (0.0%)	< 0.001	< 0.001
L-spine	Type A	26 (96.3%)	14 (73.7%)	8 (80.0%)	0.068	1
	Type B	21 (77.8%)	11 (57.9%)	6 (60.0%)	0.199	1
	Type C	11 (40.7%)	14 (73.7%)	6 (60.0%)	0.038	0.675
	Type D	0 (0.0%)	5 (26.3%)	0 (0.0%)	0.008	0.134

HC = healthy controls; MPR = multiplanar reconstruction; MRM = magnetic resonance myelography; SIH = spontaneous intracranial hypotension; SIH-R = spontaneous intracranial hypotension after recovery.

Table 4
Comparison of grades in 3D MIP images and types in thin-slice axial MPR images across groups from Readers 1 and 2.

	Grade 0	Grade 1	Grade 2	Grade 3
Reader 1				
Type A	8	0	0	0
Type B	15	39	7	2
Type C	2	11	26	3
Type D	0	0	8	17
Reader 2				
Type A	7	0	4	0
Type B	7	44	9	0
Type C	2	11	27	4
Type D	0	0	7	16

Table 5
Sensitivity, specificity, negative predictive value (NPV), and positive predictive value (PPV) from Readers 1 and 2.

	Sensitivity (%)	Specificity (%)	NPV (%)	PPV (%)
Reader 1				
Grade 3	73.7	100	84.4	100
Type D	84.2	100	90	100
Type D + Type C (T-spine)	94.7	77.8	95.5	75
Reader 2				
Grade 3	94.7	100	96.4	100
Type D	84.2	100	90	100
Type D + Type C (T-spine)	100	70.4	100	70.4

NPV = negative predictive value; PPV = positive predictive value.

and also more frequent in the SIH group than in the SIH-R group at the T-spine.

3.2. Comparison of 3D MIP and thin-slice axial MPR MRM images

The relationship between the grades of 3D MIP images and the patterns of thin-slice axial MPR of MRM images is shown in Table 4. For both readers, Types A−D on thin-slice axial MPR classification appeared to correspond to Grades 0−3 on 3D MIP system, respectively.

3.3. Epidural fluid

Epidural fluid was observed only in the SIH group and was significantly different than in the HC group at all spinal segments and at C1-2. As shown in Table 5, using “Grade 3”, “Type D”, or “Type D and Type C at T-spine” as the diagnostic criteria of CSF leakage yielded > 70% sensitivity, specificity, negative predictive value (NPV), and positive predictive value (PPV).

3.4. Case demonstration

The MRM images of two patients are shown in Figs. 3 and 4. At the onset of disease, both images showed Type D on thin-slice axial MPR MRM images and Grade 3 on 3D MIP MRM images, suggestive of positive findings of SIH. After effective EBP treatment, these findings disappeared, as confirmed by follow-up MRM images at the same levels.

4. Discussion

Orthostatic headache and CSF leakage at the level of the spine, particularly the thoracic spine,[12] are core features of SIH. However, there is considerable variability in clinical manifestations,[12] and definite diagnosis of SIH remains a challenge. Brain MRI findings indicating SIH include diffuse pachymeningeal enhancement, descent of the cerebellar tonsil, brain stem sagging, enlargement of the pituitary gland, and subdural fluid collection. Spinal MRI findings include distention of the epidural veins, epidural fluid collection, and abnormal visualization of the nerve root sleeve. The sensitivities for SIH on spinal and brain MRI are 94% and 83%, respectively, making spinal MRI more useful for diagnosis, especially in the early stage.[9]

Detection of CSF leakage at the spinal level is crucial to diagnose SIH and guide EBP. CTM and RIC are imaging modalities that can detect spinal CSF leakage, but may yield false negatives.[5] Digital subtraction myelography or dynamic CTM have been used to localize rapid CSF leaks, and MRM with intrathecal contrast administration has been applied for patients with elevated clinical suspicion of spinal CSF leak for whom conventional CTM failed.[13−16] Unfortunately, these techniques are limited due to invasiveness and radiation.

MRM is a heavily T2-weighted technique, which clarifies CSF signals to detect the pooling of CSF leakage. It is comparable to RIC[6] and more sensitive than CTM[5] in detecting leaks, and it is radiation-free and noninvasive. Therefore, MRM is recommended as the first-line imaging modality for diagnosis of spinal CSF leakage, and other imaging modalities are reserved for cases that are clinically regarded as false negatives on MRM.[6] However, intraobserver and interobserver discrepancies in MRM interpretation may occur due to unclear definition of the CSF leak.[10] There is only one report in the literature[6] that defines grading of 2D MIP MRM for CSF leakage in SIH patients, but not of axial MPR MRM, which is regarded as very important for treatment planning. In addition, this prior report did not include healthy controls for comparison. To identify the most reliable CSF distribution pattern of spinal CSF leakage, our study compared 3D MIP MRM and axial MPRMRM in SIH patients before and after effective treatment, relative to healthy controls. To our knowledge, this is the first study to investigate the CSF distribution pattern on axial MPRMRM.

T2-weighted 3D-SPACE pulse sequence was used for spinal MRM imaging in this study. It consists of variable flip angle pulses < 180°, allowing for long echo trains and short echo spacing. The parallel imaging technique of GRAPPA was also applied to reduce the acquisition time. The 3D-SPACE sequence can provide very thin, high-resolution multi-planar or oblique reformatted slices from isotropic volumetric acquisition in a reasonable time.[17]

In previous studies of spinal CSF leakage,[6,7,18] MRM was usually performed by 2D MIP imaging in either the coronal or

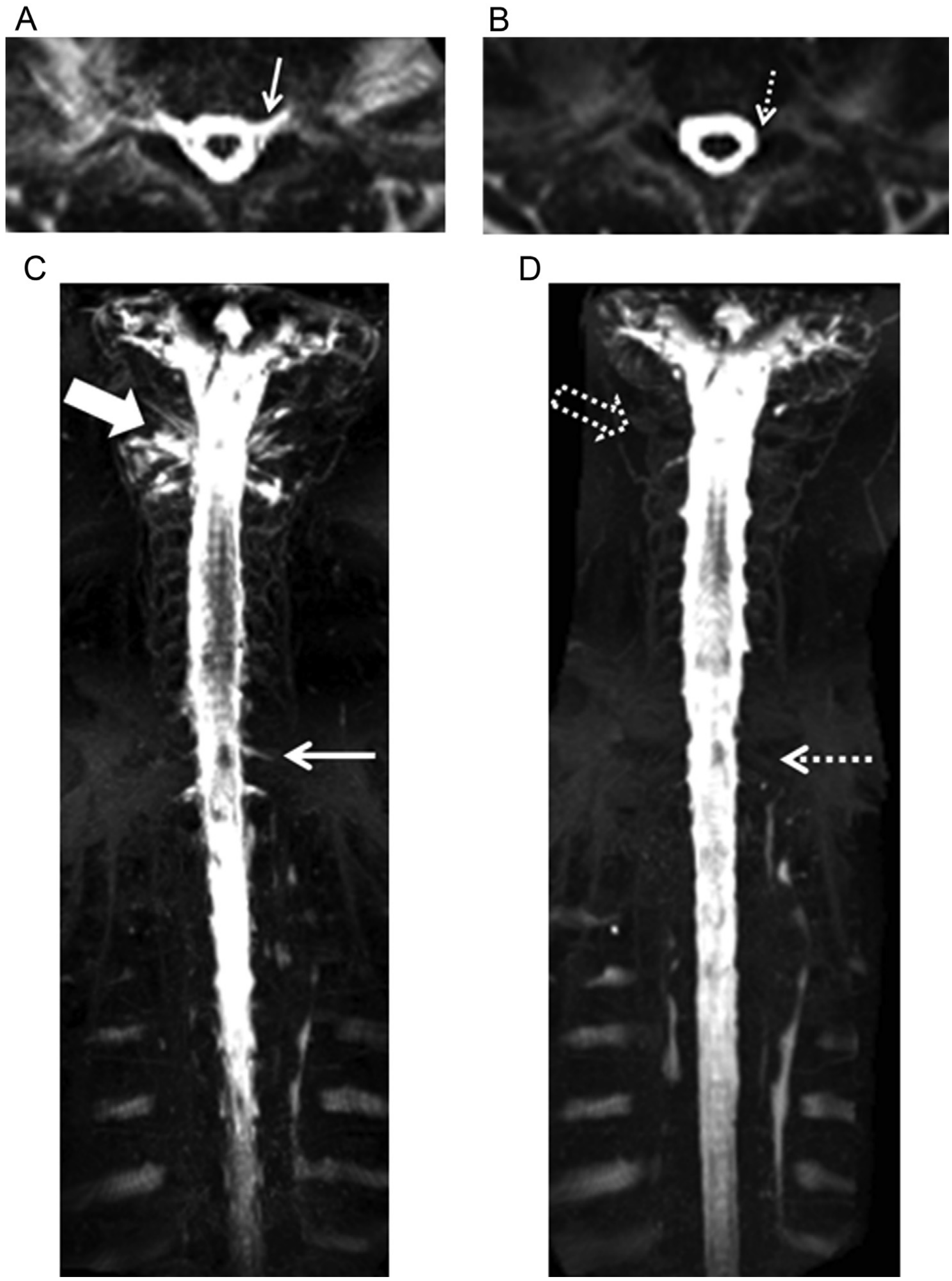

Fig. 3. A 34-year-old female who presented with orthostatic headache and was diagnosed with SIH. (A, B) Thin-slice axial MPR image of MRM at T1-2 level. CSF distribution was assessed as Type D (3A, arrow) initially and Type A 3B, broken arrow) after recovery. (C, D) Three-dimensional MIP MRM of C- and upper T-spine in the same patient. CSF distribution of T-spine was assessed as Grade 3 (3C, arrow) initially and Grade 0 (3D, broken arrow) after recovery. Notice also that epidural fluid (3C, thick arrow) at C1-2 was observed initially, but disappeared (3D, broken thick arrow) after successful treatment. CSF = cerebrospinal fluid; MPR = multiplanar reconstruction; MRM = magnetic resonance myelography.

oblique sagittal planes. Coronal MIP MRM image can show a panoramic view of the entire spine to more expeditiously detect CSF leakage sites. However, leakage within the dural sac might not be clearly defined due to a motion artifact, a very narrow primary leakage site,[18] or being obscured by surrounding structures, such as intercostal vessels or pleural effusion. Therefore, thin-slice axial MPR MRM would be necessary to delineate the exact site of leakage, in addition to 2D MIP MRM.[7,10,18] One previous study by Tomoda et al[19] used 3D fast spin-echo coronal MRM to detect CSF leakage in L-spine, demonstrating that axial MPR MRM images seemed more sensitive than reconstruction MIP images. The 3D-SPACE sequence has the advantage of offering both multiplanar thin-slice MRM and 3D MIP images of the entire spine with a reasonable acquisition time. Moreover, 3D MIP MRM has less interference from surrounding structures relative to 2D MIP MRM. The 3D SPACE combines high spatial resolution and reasonable contrast resolution with a high resilience to artifacts, making it feasible for evaluation of complex anatomy.[20] Therefore, 3D-SPACE MRM is more feasible and

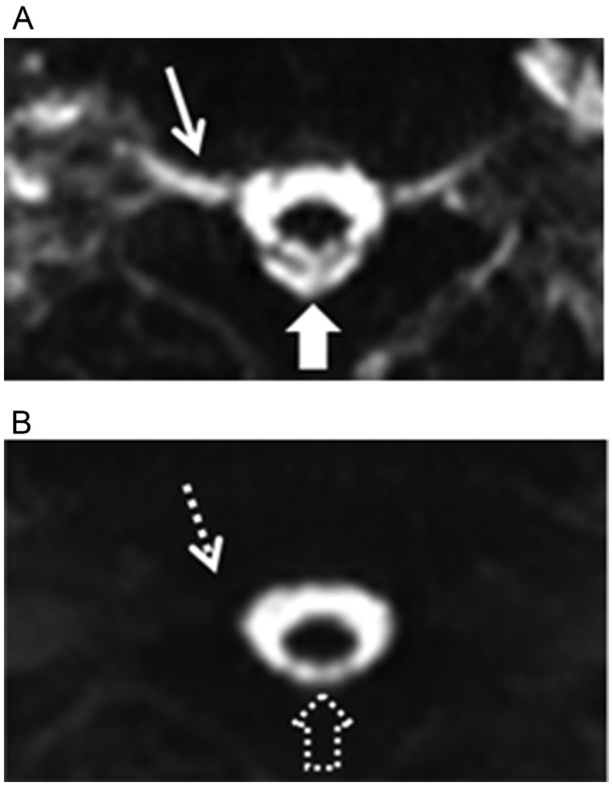

Fig. 4. A 56-year-old male who had chronic headache for many years with irregular pharmacological treatment.(A) CSF distribution on the thin-slice axial MPR image of MRM at T4-5 level was assessed as Type D (arrow) with epidural fluid (thick arrow) initially. (B) After effective EBP treatment, he was assessed as Type B (broken arrow) without epidural fluid (broken thick arrow). EBP = epidural blood patch.

accurate to detect CSF leakage than is 2D MIP MRM alone or combined with axial T2WI.

In our study, using the new grading system of axial MPR MRM, interobserver agreement between the two readers was good in SIH patients. Using the grading system of 3D MIP MRM proposed by Yoo et al,[6] interobserver agreement was good in SIH patients and moderate in HC participants. This grading system may help radiologists to categorize MRM images during clinical practice with high consistency despite different levels of experience.

In this study, Grade 3 of MIP images and Type D of MPR images, as well as epidural fluid, were noted only in SIH patients. None of these imaging presentations were noted in HC or SIH-R groups. Therefore, these findings can be considered definite criteria for CSF leakage.

In MIP MRM images, the previous literature considered Grade 1−3 as possible, probable, and definite leaks, respectively.[6] Similar to previous studies,[6,10] our study viewed Grade 3 as a definite leak, which was significantly more common in SIH patients than HC participants at C- and T-spine according to both readers, and at the L-spine according to Reader 2. CSF leakage is more frequent in the cervicothoracic junction and T-spine,[21] and the small numbers of SIH patients with L-spine CSF leakage may explain why group differences were only observed in this region for Reader 2. Grade 3 was also significantly more common in SIH patients than SIH-R patients at C- and T-spine according to Reader 1. No other significant differences were noted, possibly due to the small number of patients in SIH-R group ($N = 10$).

SIH, SIH-R, and HC groups showed no differences in Grade 2 at any segment. SIH patients had significantly less Grade 1 than HC participants at both C- and T-spine, and significantly less Grade 0 at T-spine. Therefore, Grade 2 may not be sufficient to indicate leakage, and Grades 1 and 0 do not indicate CSF leakage. In the previous study,[6] Grades 1 and 2 on 2D MIP MRM were considered possible and probable CSF leaks, respectively. These differences might result from the use of 3D images in the current study versus 2D images in the prior study; 3D differentiates discrete structures adjacent to the spinal canal, such as perineural cysts, vessels, fat, and paraspinal fluid, which might be indistinguishable from CSF leakage in 2D. Furthermore, 3D MIP MRM with rotation more accurately visualizes the length of the CSF signals arising from the thecal sac; in 2D MIP MRM, nerve root sleeves that are not parallel to the coronal plane might be underestimated.

On thin-slice axial MPR images, Type D was more prevalent in SIH patients than HC participants at all spinal segments and was more prevalent in SIH than SIH-R patients at T-spine. Type D represented the CSF leakage site as linear CSF signals radiating away from the thecal sac. Type C was more prevalent in SIH patients than in HC participants at the T- and L-spine, and was more prevalent in SIH than SIH-R patients at the T-spine. Therefore, Type C might represent a probable leak at T- and L-spine in cases of clinically-suspected SIH. On the contrary, > 70% of HC showed Types A and B patterns in all spinal segments, indicating these are not good indicators for CSF leakage.

Epidural fluid collection was a definite indicator of CSF leakage in our study, similar to other reports.[7−9]. However, merely the presence of epidural fluid did not indicate the site of leakage because it tended to be nonfocal with long segmental distribution and could be remote from the site of leakage, similar to the C1-C2 false localizing sign.[22−24]

Using "Grade 3" as the diagnostic criterion for spinal CSF leakage yielded a sensitivity of 73.7% and 94.7% for Readers 1 and 2, respectively. Reader 2 was more experienced with reading MRI than Reader 1, and might give the point of "Grade 3" more confidently. Using "Type D" as the criterion yielded a sensitivity of 84.2% for both readers. With either criterion, the specificity and PPV were 100% in both readers. Therefore, the new grading system for axial MPR MRM was more consistent than for MIP MRM, even when interpreted by a less experienced radiologist. The use of "Type D and Type C in T-spine" as the diagnostic criteria increased sensitivity to 94% and 100% for Readers 1 and 2, respectively. However, the specificity and PPV decreased to 70−80% in both readers. Therefore, caution should be used with "Type C in T-spine" as a diagnostic criterion in patients with a high suspicion of SIH. As we obtained both 3D MIP and axial MPR MRM with one image acquisition, combined grading systems for 3D MIP and axial MPR MRM could be used to achieve higher diagnostic accuracy.

There were some limitations to our study: (1) the sample size was small; and (2) no other imaging modalities or surgery were used to confirm the CSF leakage site. Further studies of larger groups and comparison of MRM with other imaging modalities could improve accuracy.

In conclusion, Grade 3 on 3D MIP, Type D on thin-slice axial MPR, and epidural fluid on MRM are definite criteria for CSF leakage, and Type C in T-spine on thin-slice axial MPR is defined as probable leakage. The 3D-SPACE sequence is feasible and accurate in whole spine MRM to detect spinal CSF leakage.

Acknowledgments

We would like to express our appreciation to the "Biostatistics Task Force of Taichung Veterans General Hospital, Taichung, Taiwan, R.O.C. for consulting on statistical analysis. Furthermore, we would like to acknowledge the participants who volunteered to participate and the MRI technologists for their assistance in data collection.

References

1. Schievink WI, Maya MM, Moser F, Tourje J, Torbati S. Frequency of spontaneous intracranial hypotension in the emergency department. *J Headache Pain* 2007;**8**:325−8.
2. Urbach H. Intracranial hypotension: clinical presentation, imaging findings, and imaging-guided therapy. *Curr Opin Neurol* 2014;**27**:414−24.
3. Schievink WI, Maya MM, Louy C, Moser FG, Tourje J. Diagnostic criteria for spontaneous spinal CSF leaks and intracranial hypotension. *Am J Neuroradiol* 2008;**29**:853−6.
4. Mokri B. Spontaneous low pressure, low CSF volume headaches: spontaneous CSF leaks. *Headache* 2013;**53**:1034−53.
5. Albes G, Weng H, Horvath D, Musahl C, Bazner H, Henkes H. Detection and treatment of spinal CSF leaks in idiopathic intracranial hypotension. *Neuroradiology* 2012;**54**:1367−73.
6. Yoo HM, Kim SJ, Choi CG, Lee DH, Lee JH, Suh DC, et al. Detection of CSF leak in spinal CSF leak syndrome using MR myelography: correlation with radioisotope cisternography. *Am J Neuroradiol* 2008;**29**:649−54.
7. Wang YF, Lirng JF, Fuh JL, Hseu SS, Wang SJ. Heavily T2-weighted MR myelography versus CT myelography in spontaneous intracranial hypotension. *Neurology* 2009;**73**:1892−8.
8. Chiapparini L, Farina L, D'Incerti L, Erbetta A, Pareyson D, Carriero MR, et al. Spinal radiological findings in nine patients with spontaneous intracranial hypotension. *Neuroradiology* 2002;**44**:143−52.
9. Watanabe A, Horikoshi T, Uchida M, Koizumi H, Yagishita T, Kinouchi H. Diagnostic value of spinal MR imaging in spontaneous intracranial hypotension syndrome. *Am J Neuroradiol* 2009;**30**:147−51.
10. Chen CH, Chen HC, Chai JW, Chen CC. Imaging appearance of magnetic resonance myelography in normal population: employing three-dimensional sampling perfection with application optimized contrasts using different flip-angle evolutions (3D-SPACE) sequence. *J Radiol Sci* 2014;**39**:1−6.
11. Headache Classification Committee of the International Headache Society (IHS). The International Classification of Headache Disorders, 3rd edition (beta version). *Cephalalgia* 2013;**33**:629−808.
12. Mokri B. Headaches caused by decreased intracranial pressure: diagnosis and management. *Curr Opin Neurol* 2003;**16**:319−26.
13. Schievink WI. Novel neuroimaging modalities in the evaluation of spontaneous cerebrospinal fluid leaks. *Curr Neurol Neurosci Rep* 2013;**13**:358.
14. Luetmer PH, Mokri B. Dynamic CT myelography: a technique for localizing high-flow spinal cerebrospinal fluid leaks. *Am J Neuroradiol* 2003;**24**:1711−4.
15. Hoxworth JM, Trentman TL, Kotsenas AL, Thielen KR, Nelson KD, Dodick DW. The role of digital subtraction myelography in the diagnosis and localization of spontaneous spinal CSF leaks. *Am J Roentgenol* 2012;**199**:649−53.
16. Akbar JJ, Luetmer PH, Schwartz KM, Hunt CH, Diehn FE, Eckel LJ. The role of MR myelography with intrathecal gadolinium in localization of spinal CSF leaks in patients with spontaneous intracranial hypotension. *Am J Neuroradiol* 2012;**33**:535−40.
17. Algin O, Turkbey B. Evaluation of aqueductal stenosis by 3D sampling perfection with application-optimized contrasts using different flip angle evolutions sequence: preliminary results with 3T MR imaging. *Am J Neuroradiol* 2012;**33**:740−6.
18. Matsumura A, Anno I, Kimura H, Ishikawa E, Nose T. Diagnosis of spontaneous intracranial hypotension by using magnetic resonance myelography. Case report. *J Neurosurg* 2000;**92**:873−6.
19. Tomoda Y, Korogi Y, Aoki T, Morioka T, Takahashi H, Ohno M, et al. Detection of cerebrospinal fluid leakage: initial experience with three-dimensional fast spin−echo magnetic resonance myelography. *Acta Radiol* 2008;**49**:197−203.
20. Tins B, Cassar-Pullicino V, Haddaway M, Nachtrab U. Three-dimensional sampling perfection with application-optimised contrasts using a different flip angle evolutions sequence for routine imaging of the spine: preliminary experience. *Br J Radiol* 2012;**85**:e480−9.
21. Schievink WI. Spontaneous spinal cerebrospinal fluid leaks and intracranial hypotension. *JAMA* 2006;**295**:2286−96.
22. Schievink WI, Maya MM, Tourje J. False localizing sign of C1-2 cerebrospinal fluid leak in spontaneous intracranial hypotension. *J Neurosurg* 2004;**100**:639−44.
23. Morgan JT, Scumpia AJ, Johnson AA, Schneider SJ. Case report: spontaneous intracranial hypotension in association with the presence of a false localizing C1-C2 cerebrospinal fluid leak. *Surg Neurol* 2008;**70**:539−44.
24. Medina JH, Abrams K, Falcone S, Bhatia RG. Spinal imaging findings in spontaneous intracranial hypotension. *Am J Roentgenol* 2010;**195**:459−64.